Volume 10, Issue 3, 2020, 5599 - 5609 ISSN 2069-5837

Biointerface Research in Applied Chemistry

www.BiointerfaceResearch.com

https://doi.org/10.33263/BRIAC103.599609

Original Research Article Open Access Journal

Received: 02.03.2020 / Revised: 26.03.2020 / Accepted: 26.03.2020 / Published on-line: 29.03.2020

Simultaneous detection of dopamine, tyrosine and ascorbic acid using NiO/graphene modified graphite electrode

Budde Kumar Swamy [1], Kudekallu Shiprath [2], Gunnam Rakesh [3], K. Venkata Ratnam [2], H. Manjunatha [2,*], S. Janardan [2], K. Chandra Babu Naidu [4], S. Ramesh [4], Kothamasu Suresh Babu [1], A. Ratnamala [2]

[1]Department of Humanities & Sciences, MarriLaxman Reddy Institute of Technology and Management, Hyderabad, Telangana, India
[2]Department of Chemistry, GITAM School of Sciences, GITAM (Deemed to be University), Bengaluru, Karantaka, India
[3]Department of Computer Science, GITAM School of Technology, GITAM (Deemed to be University), Bengaluru, Karantaka, India
[4]Department of Physics, GITAM School of Sciences, GITAM (Deemed to be University), Bengaluru, Karantaka, India
*Corresponding author email address: ***hanumanjunath80@gmail.com*** | Scopus ID 57188956297

ABSTRACT

In this work, an electrochemical sensor is fabricated by decorating the surface of graphite electrode with NiO/graphene (NGMG) nanoparticles and employed for the detection of dopamine (DA), tyrosine (Tyr) and ascorbic acid (AA). The structure and morphology of prepared NiO nanoparticles are examined by XRD,SEM, FTIR and Raman techniques. The electrochemical properties have been investigated by cyclic voltammetry (CV), differential pulse voltammetry (DPV) and chronoamperommety. The modified electrode is prepared by a simple drop casting method. The electrode shows good electro catalyticactivity towards oxidation of DA, Tyr and AA. It successfully separates the oxidation current signals of AA, DA and Tyr into clearly visible three distinct oxidation peaks compared to a single, overlapped oxidative peak on bare graphite electrode. The peak potential difference between AA-DA, DA-Tyr and AA-Tyr is 228 mV, 303 mV and 565 mV respectively in cyclic voltammetry (CV) studies and the corresponding peak potential separations are 243 mV, 318 mV and 561 mV respectively in differential pulse voltammetry (DPV). It is found that oxidation mechanism of DA, AA and Tyr on NGMG are different owing to a different type of interaction of the modified layer with the bio-analytes. The modified electrode, NGMG has high selectivity and sensitivity in addition to other factors like low cost, convenient and a hassle free electrochemical method for simultaneous determination of DA, AA and Tyr in their ternary mixture.

Keywords: *NiO/graphene modified graphite, Dopamine, Ascorbic acid, Tyrosine, Drop cast method, Cyclic voltammetry, Differential Pulse voltammetry and Chronoamperometry.*

1. INTRODUCTION

Over the years, significant efforts have been made in the technological development of diagnostic tools used in medicine. The present diagnostic tools have certain limitations in the early detections of certain diseases like diabetes mellitus, cancer, and neurological diseases which are often linked with metabolic disorders [1].

Dopamine, ascorbic acid and tyrosine become some of the biomarkers to analyze such diseases since their concentration level in blood isrelated to metabolic disorders. Tyrosine (Tyr) is a non essential aromatic amino acid produced by hydroxylation of phenylalanine and acts as a biochemical precursor of dopamine and norepinephrine. It is responsible for synthesis of melanin, thyroxin, adrenaline and causative agent for genetic, hormonal and neurological disorders. In fact, a few inborn disorders like Tyrosinaemia-I, II and III type, Hawkinsinuria, and Alkpatonuria (AKU) are caused by irregularities of tyrosine metabolism [1-5].

Since tyrosine belong to catecholamine family and a neurotransmitter, its concentration is one of the controlling factors of neurological disorders like stress and mood changes. A recent report [6] published on tyrosine reveals that a high level of tyrosine in blood tissue is a litmus test to foresee and analyzes the level of certain metabolic disorders like type-2 diabetes, insulin resistance, obesity and liver cancer. A healthy human being must have a tyrosine in the concentration in the range of range of 30 – 200 μM in blood plasma. Dopamine (DA) is a hormone belonging to the family of catecholamine neurotransmitters and plays an essential role in neural transmission. Its concentration in biological fluids is pivotal and abnormal levels lead to diseases like Huntington's disease, Schizophrenia and Parkinson's disease etc [7-15].

Vitamin-C or Ascorbic acid is one of the water soluble vitamins which play a prominent role in formation of collagen, fiber and cartilage as well as it has been used for curing mental illness and scurvy. The amount of AA level in biological fluid is one of the ways of quantifying the stress level and its imbalance can lead to diabetes mellitus, cancer etc [16-18].

Though analytical methods like chromatography, fluorescence, mass spectrometry and other techniques are available for the detection of Tyr [19-22], DA [23-31] and AA [32-38] in biological fluids, they are useful to certain extent due to their own limitations. Owing to fast response, accuracy and portability, the electrochemical methods using electrochemical sensors [39] to analyze the DA, AA and Tyr coexisting in biological fluid [40-43] are very promising in accurate quantification of these bio-molecules. However, the problem with sensing of biological molecules is the inability of bare electrodes to distinguish the potentials at which these electro active species undergo oxidation and give oxidation current as analyte signal.

One of the ways to overcome this problem is to chemically modify the bare electrode surfaces. It is well known fact that for modification of bare electrode surfaces, materials like carbon, conducting polymers and metal oxide nanoparticles are very attractive owing to their ability to separate the oxidation potentials of electro active molecules and measure their concentration as a function of oxidation current. The materials used for modification should also enhance or amplify the current obtained due to the oxidation of the electro active molecules. Several modified electrodes have been used for the determination of dopamine, tyrosine and ascorbic acid making use of different materials like metal nanoparticles, conducting polymers and carbon [44-45]. NiO nanoparticles have also been used to design many electrochemical sensors to determine amino acids, neurotransmitters, sugars and other bio-molecules [46-51].

Though plenty of research on the carbon based materials is carried out, the development of electrochemical sensors using graphene, MWCT and reduced graphene etc [52-62] is still thriving the interest of researchers due to their novel properties like high surface area, excellent electrical conductivity, high mobility of charge carriers and quantum hall effect. In the present work, NiO nanoparticles are prepared by co-precipitation method and the synthesized NiO nanoparticles are characterized by XRD, Raman andIR techniques. The NiO/graphene modified graphite electrode is then used for the determination of DA, AA and Tyr in their ternary mixture simultaneously. Such work i.e. synthesis and application of NiO/graphene modified graphite electrode particularly for the simultaneous determination of DA, AA and Tyr are not reported to the best of our knowledge.

2. MATERIALS AND METHODS

2.1. Chemicals.

Nickel(II)chloride, NaOH, ethanol, dopamine, ascorbic acid, graphene and liquid paraffin were purchased from Sigma-Aldrich and used as received. Potassium chloride, potassium dihydrogen phosphate, dipotassium hydrogen phosphate, tyrosine were purchased from Fischer Scientific Ltd. and used as received. All other chemicals were of analytical grade and used without further purification. Stock solutions of 0.01M of dopamine, ascorbic acid and 0.002 M of tyrosine were prepared freshly using double distilled water. Phosphate buffer solutions (PBS) were prepared from stock solutions of 0.1M K_2HPO_4, 0.1M KH_2PO_4, 0.5 M HCl and 0.5 M NaOH.

2.2. Equipment.

The synthesised NiO nanoparticles were physically characterised by Powder X-Ray Diffraction (XRD) using X'Pert PRO Diffractometer with Cu Kα radiation of wave length 0.15406 nm. The surface morphology of the synthesised particles was observed using a scanning electron microscope (SEM) HITACHI S4160. Fourier transforms infrared (FT-IR) spectra and UV-Vis spectra (Thermo model, Instrument model λ 35) of the material were recorded to determine the functional groups. Raman spectra of the material at room temperature (RT) were obtained using 3D scanning confocal microscope with spectrometer nanofinder-S (SOLAR TII, Ltd.).

2.3. Electrochemical measurements.

The electrochemical measurements like cyclic voltammetry, differential pulse voltammetry and chronoamperometry were carried out using a potentiostat/ galvanostat, VSP, Biologic's instruments, France. A three electrode electrochemical cell consisting of NiO/Graphene modified graphite electrode as working, a platinum wire as auxiliary and a saturated calomel electrode as reference electrode was used for all electrochemical measurements with 0.1 M phosphate buffer solutions (PBS) + 0.1 M KCl as supporting electrolyte.

2.4. Synthesis of NiO nanoparticles.

Nickel oxide nanoparticles are synthesized by co-precipitation method. In a typical procedure, 2.6 g of Nickel (II) chloride was dissolved in 100 ml of distilled water. To this $NiCl_2$solution, sodium hydroxide (0.1 M NaOH) was added drop by drop under constant stirring. The resultant mixture obtained was heated at 60° C and stirred at this temperature for 8 hours. It was then refluxed at room temperature for 24 hours. The obtained green precipitate was washed with double distilled water followed by ethanol to remove any possible ionic remnants if formed. The sample was dried by heating at 90°C in air and then calcined at 250° C when greenish sample turned into dark green color.

2.5. Preparation of NiO/Graphene modified graphite electrode (NGMG).

A spectroscopic grade pure graphite (6 mm size) cylinder, purchased from Sigma Aldrich, was inserted into the hole of a teflon bar with the same internal diameter. The end of graphite electrode was polished with emery papers of different grades like 1000 and 800 until a mirror shining surface was obtained. It was then sonicated with double distilled water for two minutes. A NiO/graphene suspension was prepared by mixing 5mg of NiO nanoparticles with 5mg of graphene in 0.1 ml of liquid paraffin and 0.9 ml of water by sonicating the mixture for 30minutes. The obtained homogenous black suspension of about 10 µL was dropped on clean surface of graphite electrode and allowed for drying for about 3 hours at room temperature [63]. The resulting modified electrode acts as a working electrode and referred to as NiO/graphene modified electrode (NGMG).

3. RESULTS

3.1 Characterization.

The XRD pattern obtained for the synthesized NiO nanoparticles is as shown in Fig.1(A). The XRD pattern shows three distinct peaks at 36.5^0, 43.5^0 and 63^0 with peak line broadening at the base which is a characteristic feature of materials having nanoparticles size. It is well known that XRD peak width increases as the size of the particle decreaseindicating reduced defects in the prepared sample. No other peaks are present in XRD pattern indicating that the prepared material is phase pure. The well-defined peaks are indexed as (111), (200), (220), (311) and (222) that correspond to face-cantered cubic (FCC) structure of NiO and is in consistent with standard (JCPDS -file: 78-0429,

Fm3m space group) data. The crystallite size can be determined using Debye-Scherer's formula given as follows,

$$d = K\lambda / (\beta \cos \theta)$$

Where *d*-Size of the crystallite, K-0.9, Scherrer's constant, λ-Wavelength of the Cu-Kα radiation (1.5406 Å), β- full width at half maximum (FWHM) intensity, 2.783 and θ-43.3^0, peak position.

The average particle size of synthesized NiO material is found to be between 10-12 nm. Fig.1(B) shows the SEM image of NiO nanoparticles and it is clearly seen that the synthesised NiO nanoparticles are spherical in shape. The SEM image also reveals high agglomeration of nanoparticles leading to the formation of cluster as well as ultrafine NiO nanoparticles. This provides larger surface area imparting excellent catalytic activity for nanoparticles. The average particle size from SEM image was 19 nm.

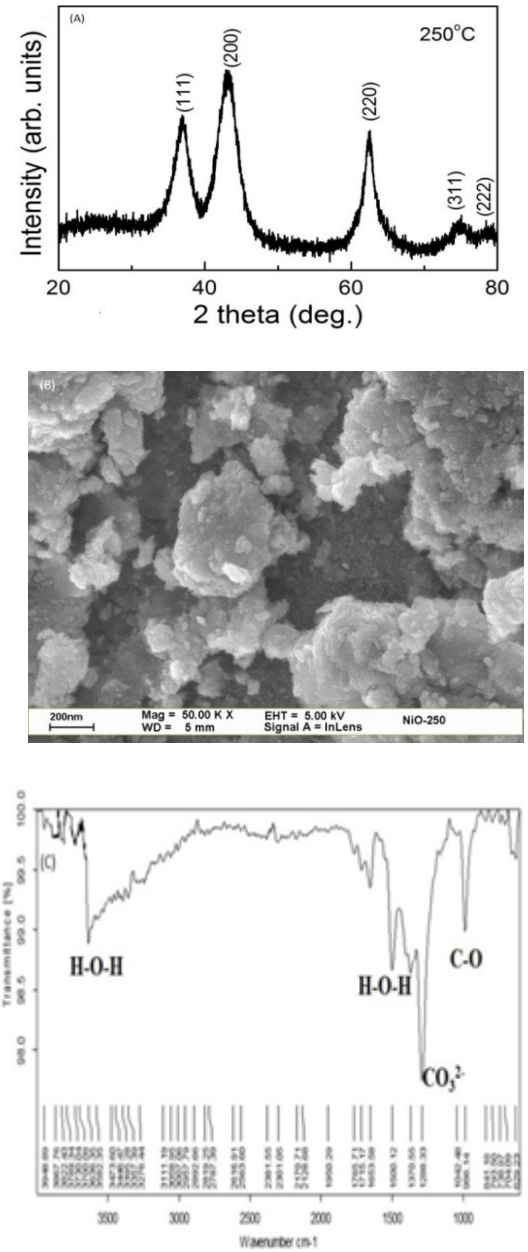

Figure 1. A) XRD pattern of NiO nano particles B)SEM image of NiO nano particles C) FTIR Spectrum of NiO nano particles

Fig. 1(C) shows the IR transmittance spectrum for NiO nanoparticles and it exhibits characteristic peaks at 590 cm^{-1} and 610 cm^{-1} which corresponds to the vibration of Ni-O nanoparticles while other two distinct peaks at 1651 cm^{-1} and 3635 cm^{-1} are attributed to H-O-H stretching indicating that sample contained traces of water[64]. The prominent peak at 1010 cm^{-1} belongs to C-O stretching and a peak at 1510 cm^{-1} confirms the presence of carbonate groups. In UV-Vis absorbance spectrum shown in Fig. 2(A), it can be seen that the strong absorption peak around 349 nm is assigned to the blue shift due to absorption by NiO nanoparticles. Fig.(2B) shows the Raman spectrum of NiO nanoparticles and it is observed that a characteristic peak around 500 cm^{-1} belongs to stretching mode of NiO [65].

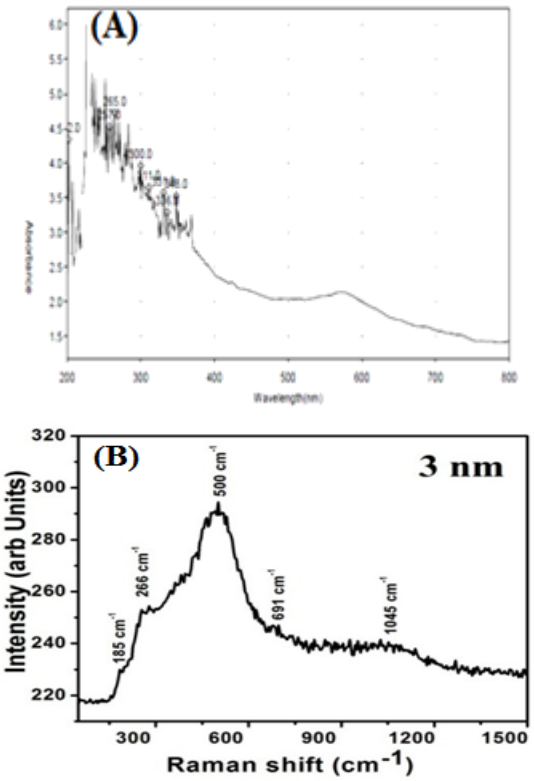

Figure 2. A)UV-spectrum of NiO nano particles B) Raman spectrum of NiO nano particles

3.2. Electrochemical oxidation of DA and Tyr in presence of AA at NiO/Graphene modified graphite.

DA and AA co-exist in the many biological fluids and interfere with each other's determination. In addition, they undergo oxidation at very close potentials on bare electrode surfaces making their analysis on bare graphite electrode difficult. Tyrosene is also present in blood and other biological fluids and its concentration are generally very low.

The high concentrations of DA and particularly AA may interfere in the determination of tyrosene. Therefore, simultaneous determination of DA, AA and Tyr is of great significance in electro analysis research. The electrochemical behaviors of AA, DA and Tyr at NGMG electrode were studied in their ternary mixture using cyclic voltammetry and differential pulse voltammetry. Fig. 3(A) shows the CV profiles recorded in PBS buffer solution, pH 7.0 containing 200 µM DA, 500 µM Tyr and 5 mM AA at NGMG electrode (e) and at bare graphite electrode (a). From the figure, it is

very clear that the oxidation peaks of AA, DA and Tyr on bare graphite electrode coalesce to appear as a single peak at a potential of 0.511 V with reduced peak current. From this, no information on the concentrations of AA, DA and Tyr can be obtained. On the other hand, at NGMG modified electrode, the oxidation peaks of AA, DA and Tyr are very well separated and the peaks appear at different potentials, 0.122V, 0.350 V and 0.653 V respectively. This indicates that the modified electrode successfully separated and distinguished the oxidation peaks of AA, DA and Tyr. The oxidation peak potential differences between AA-DA, DA-Tyr and AA-Tyr on NGMG modified electrode is found to be 228 mV, 303 mV and 565 mV respectively in cyclic voltammetry (CV) studies.

Fig.3(B) shows the DPV curves for the oxidation of 200 µM DA, 500 µM Tyr and 5 mM AA ternary mixture at NGMG electrode. It is clear from the figure that on bare graphite a single overlapped peak appears for the oxidation of all the three analytes under study. However, at the NGMG modified electrode, the oxidation peak potentials of AA, DA and Tyr are clearly seen separated and three distinct peaks appear. The peak potential separation between, AA-DA, DA-Tyr and AA-Tyr in DPV are found to be 243 mV, 318 mV and 561 mV respectively. From the above discussion, it is clear that the NGMG modified electrode has good electro-catalytic activity towards the oxidation of AA, DA and Tyr in their ternary mixture compared to that on the bare graphite electrode. This proves that the simultaneous determination of DA, Tyr is possible at the NGMG electrode in the presence of high concentration of AA.

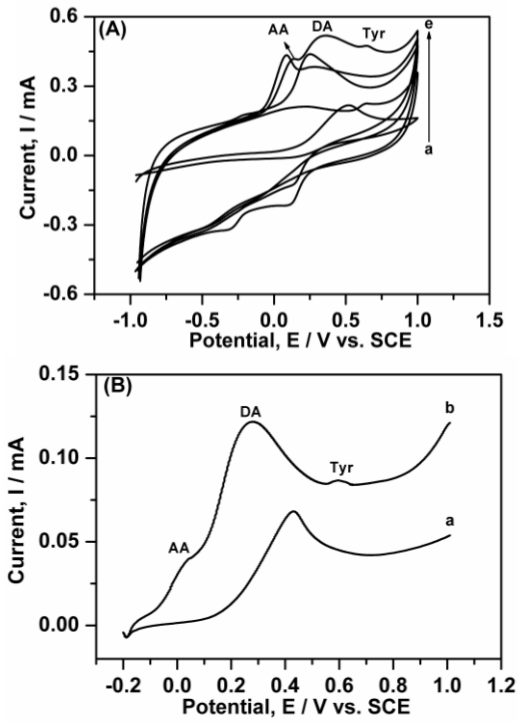

Figure 3. A) Cyclic voltammograms of a) Bare graphite with DA 200 µM, 500 µM Tyr and 5mM AA b) NGMG electrode no analyte c) NGMG electrode with 200 µM DA d) NGMG electrode with 5mM AA e) NGMG graphite with 200 µM DA, 500 µM Tyr and 5 mM AA; Scan rate 50 mV s^{-1} B) Differential pulse voltammogram of a) Bare graphite with 200 µM DA, 500 µM Tyr and 5 mM AA b) NGMG graphite with 200 µM DA, 500 µM Tyr and 5 mM AA

3.2. Electrochemical behavior of DA, Tyr and AA individually atNiO/Graphene modified graphite electrode.

Electrochemical oxidation of DA, AA and Tyr were studied using NiO/Gr modified graphite electrode by cyclic voltametry. The measurements are done in presence of 500µM of DA, 5mM of AA and 500 µM of Tyrosine individually at NiO/graphene modified graphite electrode (NGMG) and results are compared with that on bare graphite electrode. All experiments were performed at neutral conditions using phosphate buffer solution (PBS, pH=7.0) due to the fact that all these coexist in biological fluids at neutral pH.

3.2.1. Electrochemical studies of DA at the NiO/Graphene modified Graphite electrode (NGMG).

Fig. 4(A) shows the cyclic voltammogram of 250 µM DA at bare graphite electrode (2) and at NGMG electrode (4) in PBS (pH=7.0) solution. In the absence of DA, the bare graphite electrode exhibits no obvious oxidation and reduction peaks in PBS, pH 7.0 solution (a) and the NGMG modified electrode shows an anodic peak at 0.241V and a cathodic peak at 0.126V corresponding to oxidation and reduction of Ni^{+2}/Ni^{+3} redox couple of NiO nanoparticles respectively(c). On the other hand, DA undergoes reversible oxidation and reduction at bare graphite electrode with an oxidation peak located at about 0.257 V (b) and at the modified electrode, its oxidation peak is observed at 0.204 V. The oxidation peak potential of DA at NGMG modified electrode shifted towards negative side by around 60 mV compared to that at the bare graphite. In addition, there is significant enhanced of oxidation peak current on the modified electrode indicating better electro catalytic behavior of NiO/Graphene nanoparticles towards DA oxidation. The oxidation peak at +0.204 V on the CV curve of DA at the modified electrode is assigned to the formation of dopaminoquinone (DA^+) (product of dopamine oxidation) and the cathodic peak at +0.125V is assigned to the reduction of DA^+ to leucodopanoquinone [66]. Fig. 4(B) shows the CV profiles of DA at different concentrations and it is clear from the figure that the oxidation current of DA increases linearly with an increase in concentration at the NGMG modified electrode. The additional cathodic peak observed at 0.280 V is attributed to the reduced species of dopaminequinone in the solution [67].

3.2.1.1. Effect of scan rate.

To understand the electron transfer kinetics of DA oxidation at NGMG, CV profiles were recorded at different scan rates starting from 50 to 400 mV s^{-1} and are as shown in Fig. 4(C). From the figure, it is found that the peak potentials shift as the scan rates are varied. A plot of peak current (I_{pa}) against the square root of scan rate ($\upsilon^{1/2}$) (inset in the figure) shows a linear relationship with almost zero intercept confirming a diffusion-controlled process [68]. The linear relationship between peak current and square root of scan rate confirms that the modified layer NiO/graphene is electroactive, conducting and confined to the surface. In order to find the kinetic parameter, charge transfer coefficient (α), E_{pa} vs. log υ graph was plotted and is as shown in Fig. 4C (inset). The slope of the linear equation of E_{pa} vs. log υ plot is equal to $-2.303RT/(1-\alpha)nF$ and is used to determine the kinetic parameter, α; where *R, T* and *F* are the molar gas constant, temperature and faraday constant. From the linear regression relation, E_{pa} =0.033log υ +0.163 obtained for the plot of E_{pa} vs. log υ, the anodic charge transfer coefficient (α) was calculated to be 0.104. The calculated Tafel slope or NGMG electrode is found to be 0.066 V dec^{-1} whichis less than theoretical value of 0.118 V

dec^{-1} for an one electron process suggesting no adsorption of dopamine occurs on the electrode surface. Also electron transfer rate constant (k_s) calculated using Laviron's equation [69-70] (eq. 1) for the NGMG electrode was around 0.28 s^{-1} at 0.05 V s^{-1}.

$\log k_s = \alpha \log(1-\alpha) + (1-\alpha)\log\alpha - \log(RT/nF n) - \alpha(1-\alpha) nFE/2.3RT$------- (1)

According to the kinetics of electrode process, if rate constant is greater than0.01 s^{-1}, the electron transfer process is fast and reversible. Thus the oxidation of DA at NGMG electrode is fast, reversible and diffusion controlled with a two proton coupled two electron processes.

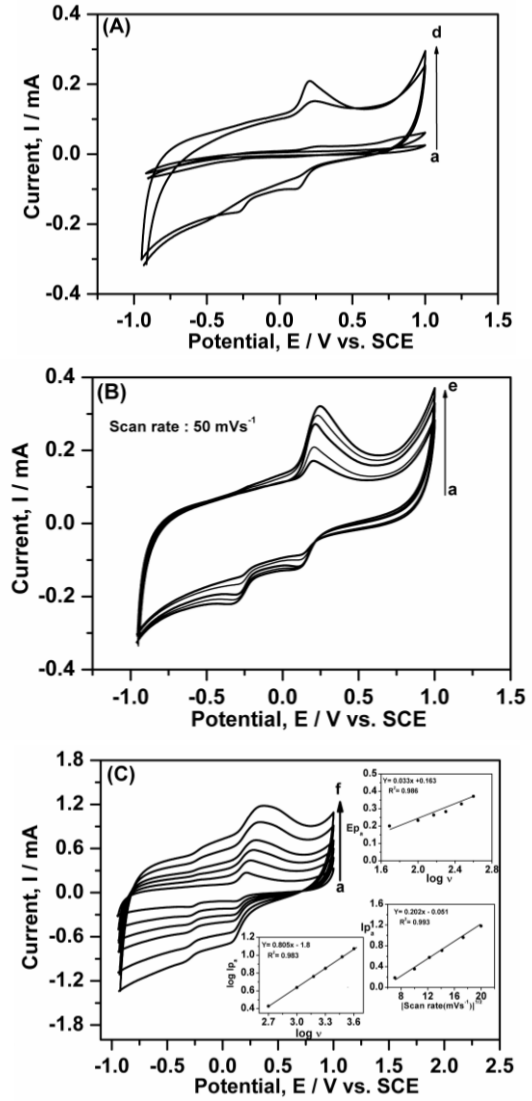

Figure 4. A) Cyclic voltammograms of: a) Bare graphite b) Bare graphite with 250 µM DA c) NGMG electrod) NGMG with 250 µM DA: Electrolyte solution 0.1M Phosphate buffer solution (pH 7.0) + 0.1M KCl B) Cyclic voltammograms of DA of various concentrations at NGMG electrode: a)125 µM b)250 µM c)500 µM d)1 mM. Scan rate: 50 mV s^{-1}C) Cyclic voltammograms of 500 µM DA at NGMG electrode at different scan rates a) 50 b)100 c)150 d)200 e)300 f) 400 mV s^{-1} Inset: plots of E_{pa} vs log υ and log I_{pa}vs log υ and I_{pa} vs. υ $^{1/2}$

3.2.1.2. Effect of pH.

In most of the cases, the pH is an important factor concerning electrochemical reaction. The dopamine undergoes structural changes with change in pH of the solution and is studied by cyclic voltammetry. Fig. 5 shows the CV profiles of DA NGMG electrode in PBS solutions of different pH ranging from 3-11 at a scan rate of 50 mV s^{-1} at. In acidic media (between pH 3-6), high anodic peak currents were observed and in basic media(above pH 8), the anodic current peak decreases. At pH 7.5, the anodic peak current is highest and has biological environment for detection of DA. As the pH increases, the anodic and cathodic peak potential shifts to more negative potential indicating that dopamine oxidation is easier with decreasing pH and combined with proton coupled electron transfer reaction. When the pH is around 7.5 DA exists in deprotonated state (DA^{-2}) and undergoes oxidation with higher kinetic rates [71-72]. This might be due to the formation of NiOOH which oxidizes the DA to dopaminequinone and reaction as follows [73]

$$NiO + OH^- \longrightarrow NiOOH + H_2O + e^-$$

The value of proton involved in electrochemical oxidation of DA can be obtained using the following equation:

$$E_p = E^o - 0.059p/n\text{pH}$$

Where,*p*-the value of proton in the electrode reaction and *n*-number of electrons involved in the reaction. Based on the above equation, good linearity was found between $E_p$and pHwith a slope of 0.0593 (see Fig.5 inset) suggesting that the number of protons is equal to number electrons participated in electrochemical oxidation of DA at NGMG [74]. The possible reaction for DA as follows:

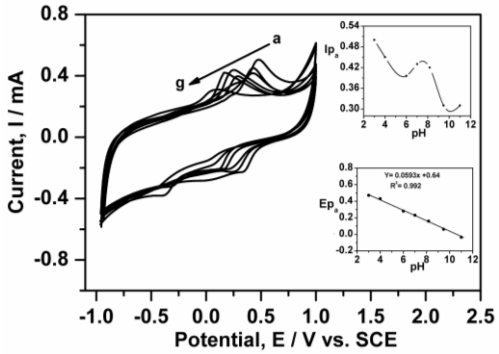

Figure 5. Cyclic voltammogram of 500 µM DA at NGMG of different pH in 0.1M PBS (a-g);a)3.0 b) 4.0 c) 6.0 d) 7.0 e) 8.18 f) 9.48 g)11.0 Inset plots I_{pa} vs. pH and E_{pa} vs pH.

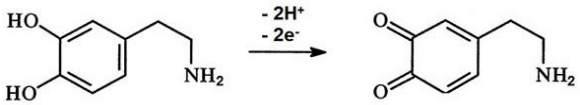

Figure 6. Oxidation reaction of DA(two electron transfer)

3.2.2. Electrochemical studies of AA at the NiO/graphenemodified Graphite electrode (NGMG).

Fig. 8(A) shows the electrochemical behavior of 5mM AA at NGMG in PBS, pH 7.0 solution. The CV profile of AA at NGMG shows an irreversible oxidation with an anodic peak potential at 0.089 V (d). However, on bare graphite electrode (a), AA undergoes oxidation at a potential of 0.408 V and on the NiO modified graphite electrode(c) the oxidation is observed at 0.241 V. It is very clear that the oxidation peak potential of AA shifted towards negative side by about 150 mV. A strong negative shift in the peak potential and an enhancement of anodic peak current

indicates that AA undergoes oxidation on NGMG modified electrode easily than on the bare graphite electrode. Fig. 8(B) shows the CV profile of AA at different increasing concentrations and a plot of anodic peak current vs. concentration shows a linear relationship. The effect of scan rate on the oxidation reaction of 5mM AA was also studied in the range 50 to 400 mV s^{-1}) and is as shown in Fig. 8(C). From Randels- Sevcik equation, a good linear relation is obtained between I_{pa} and $\upsilon^{1/2}$ with zero intercepts, I_{pa}= 0.071$\upsilon^{1/2}$ – 0.35, indicating that it is a diffusion controlled process(Fig. 8(C), inset). A plot of E_{pa} vs. logυ was also drawn to evaluate the kinetic parameters like charge transfer coefficient (α) and Tafel value (graph not shown). The linear plot obtained gives a slope of 0.128 which upon calculation gives a charge transfer coefficient (α) of 0.769. The Tafel value was found to be 0.256 V $dec^{-1}$and is relativelyhigher than the theoretical value of 0.118 V dec^{-1} for one electron transfer process and indicates that reaction seems to be proceeding through surface adsorption of chargedintermediates species. A plot log I_{pa} vs. log υ (Fig. 8(C), inset) with a unit slope confirms that reaction proceeds through the formation of some adsorbed species at the surface of the electrode. The possible mechanism of electrochemical oxidation of AA is as follows:

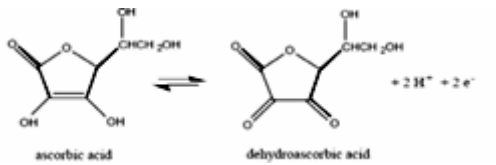

Figure 7. Oxidation reaction of AA

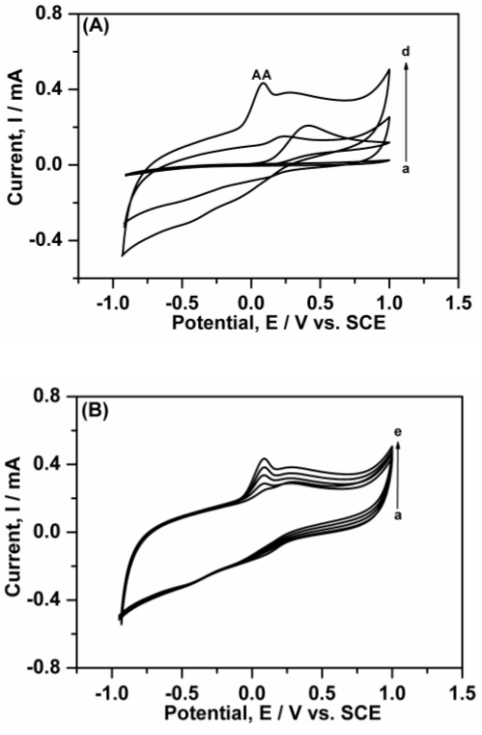

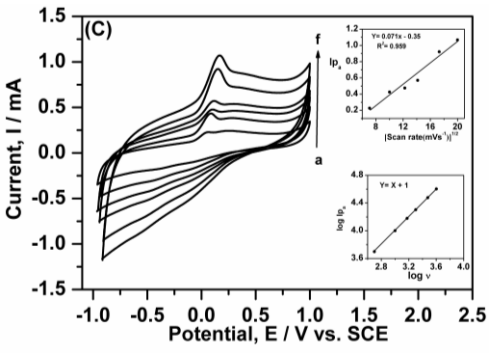

Figure 8. A) Cyclic voltammogramsof a) Bare graphite b) Bare graphite with 5 mM AA c) NGMG electrode in 0.1 MPBS, pH 7.0 d) NGMG with 5 mM AA in 0.1M Phosphate buffer solution (pH 7.0) + 0.1M KCl B) Cyclic voltammograms of various concentrations AA at NGMG electrode; a)1 mM b)2 mM, 3)3 mM 4) 4 mm & 5)5 mM.Scan rate: 100 mV $s^{-1}$and C) Cyclic voltammograms of 5 mM AA at NGMG electrode at different scan rates; a) 50 b)100 c)150 d)200 e) 300 f) 400 mV s^{-1}, Inset plots of I_{pa} vs. $\upsilon^{1/2}$ and log I_{pa} vs. logυ

3.2.3. Electrochemical studies of L-Tyrosine at NGMG.

Fig. 9 (A) shows the cyclic voltammetry studies Tyr at NGMG modified electrode in PBS solution. On bare graphite electrode, Tyr undergoes irreversible oxidation with the anodic peak located at 0.804 V (b). On the other hand, on NGMG modified electrode, it undergoes irreversible oxidation with the anodic peak located at 0.621 V with an enhanced peak current.

The shift in oxidation peak potential and enhancement in the anodic peak current suggests that the NGMG electrode shows good electro catalytic activity towards try detection. In order to determine the effect of scan rate, cyclic voltammetry profiles were recorded at NGMG in PBS 7.0 solution containing **5**00 µM tyrosine and are as shown in Fig. 9(B). Using *Randels- Sevcik* equation , a plot of I_{pa} verses square root of scan rate (50 to 400 mV s^{-1}) shows good a linear relationship with zero intercept, I_{pa} = 0.040$\upsilon^{1/2}$ - 0.166 (inset in Fig. 6(B). This suggests a diffusion controlled process for the oxidation of Tyr at NGMG electrode.

The electrochemistry of surface- adsorbed species like inactive complexes or intermediates [75] were also confirmed from the slope of 0.879 in the log I_{pa} vs. logυ shown in inset of Fig. 9(B) according to the linear equation ; log I_{pa} = 0.879 logυ – 2.3. The charge transfer coefficient (α) was calculated from slope of the plot of E_{pa} vs. log$\upsilon$with a linear regression equation, E_{pa} = 0.112logυ + 0.425 (graph not shown). The charge transfer coefficient (α) for NGMG electrode in the presence of tyrosine was found to be 0.485 and estimated Tafel slope (b) was 0.23 Vdec^{-1}.

The obtained results are correlated to theoretical value of charge transfer coefficient (α) for diffused controlled process i. e 0.5 and that of Tafel value the rate determining step of one electron process is 0.118V dec^{-1}. The high Tafel value indicates adsorption of reactants or intermediates on the electrode surfaces or into the porous electrode. So electrochemical oxidation of Tyr at NGMG electrode is diffusion controlled process with some adsorbed species making the process sluggish and exhibits irreversibility.

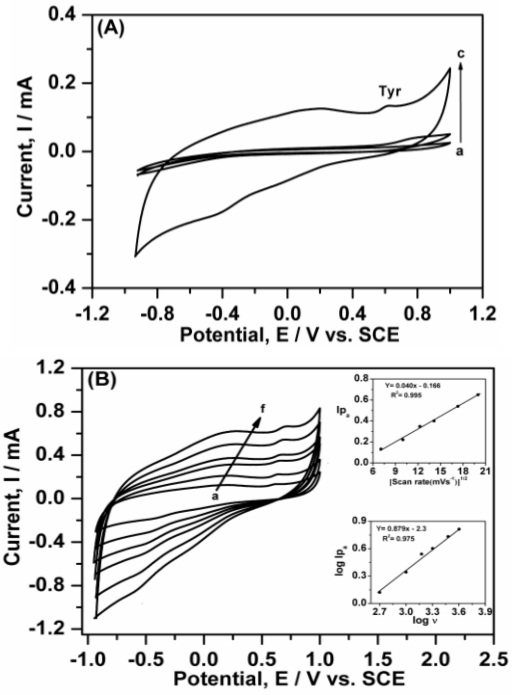

Figure 9. A) Cyclic voltammograms of a) Bare graphite electrode b) Bare graphite with 500µM Tyr c) NGMG electrode with 500 µM Tyr solution 0.1M Phosphate buffer solution (pH 7.0) 0.1M KCl B) Cyclic voltammograms of 500 µM Tyr at NGMG electrode at different scan rates a)50 b) 100 c)150 d)200 e)300 f) 400 mV s^{-1} Inset plots; Plot of I_{pa} vs. $\upsilon^{1/2}$ and log I_{pa} vs. log υ.

3.3. Selective determination of DA in the presence of tyrosine and ascorbic acid at NGMG.

DA and Tyr have similar structures and coexist in biological fluids. In addition, they undergo oxidation at close potentials on bare electrodes and the determination of one in presence of the other becomes significant for researchers. The cyclic voltammetry studies were conducted in a binary mixture containing a constant concentration of tyrosine (500µM) and varying concentration of DA was shown in Fig. 10(A). In another experiment, cyclic voltammetry profiles were measured in a binary mixture containing a constant concentration of AA and varying concentration of DA at the NGMG in PBS solution (graph not shown). The cyclic voltammetry results of the studies are given in Table 1. From the peak potential and peak current values from the Table 1, it is clear that it is impossible to deduce any information about the concentration of analytes on bare graphite since anodic peaks coalesce broad peak. On other hand, at NGMG electrode, a remarkable difference between oxidation peak potential of two analytes, DA-AA or DA-Tyr was observed. Peak potential difference of about 397 mV and 194 mV for DA -Tyr and AA-DA respectively proves that the NGMG electrode has a better electro-catalytic activity for selective identification of DA in biological fluids.

3.4. Selective determination of Tyrosine in the presence of ascorbic acid at NGMG electrode.

The cyclic voltammetry curves of binary mixture containing tyrosine and AA on bare graphite (Fig. not shown) shows a solitary anodic peak which cannot yield any information about the amount of the two analytes. However, on the modified electrode two distinct peaks for AA and tyrosine are clearly visible and the results of the studies are tabulated in table-2. From table 2 it is clear that there is a significant enhancement in the anodic peak current (I_{pa}) for AA and Tyr at the NGMG modified electrode compared to that at the graphite electrode. Also, a prominent peak potential difference of 586 mV between AA and Tyr clearly indicates that tyrosine can be determined in the presence of a high concentration of AA.

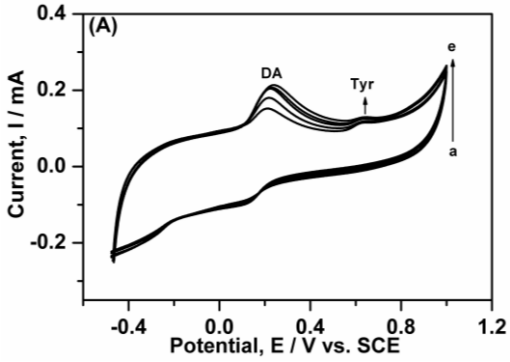

Figure 10.A) Cyclic voltammograms of variation of concentration of DA a) 100 b) 200 c) 300 d) 400 e) 500 µM ; Concentration of Tyr- 500 µM at NGMG electrode: Electrolye solution 0.1 M Phosphate buffer solution. (pH 7.0) + 0.1 M KCl : Scan rate 50 mV s^{-1}

3.5.Amperometric studies of DA and AA using NGMG electrode.

In order to find out the sensitivity of the NGMG electrode, the electrochemical studies have been continued with detection of DA and AA using chronoamperometry since this experiment under stirred conditions has much higher current sensitivity than cyclic voltammetry. Furthermore, this was also meant to determine the detection limit of DA and AA at the NGMG electrode.In separate experiments a given volume of DA and AA were adding into stirring 0.1M PBS solution (pH 7.0), the NGMG responded swiftly and the current increases sharply to reach a steady value.

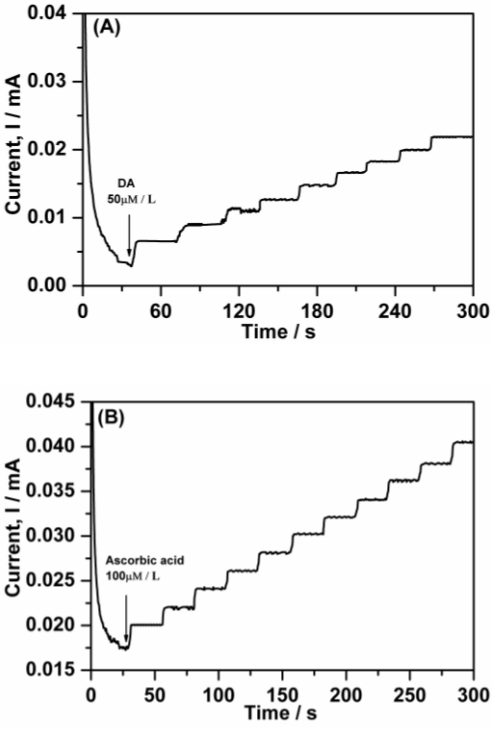

Figure 11. Amperometric response of NGMG in 0.1 M PBS, pH 7.0 for, A) each addition of 50 mM UA and the current was measured at constant applied potential of 300 mV and B) each addition of 50 mM AA and the current was measured at a constant applied potential of 120 mV

To maintain homogeneity of the solution, a magnetic stirrer was used with 100RPM. In case of DA, Figure 11(A) shows the amperogram at NGMG electrode for successive additions of 50 µM DA which indicates linear increase in measured currents with each addition of 50µM DA. As well as a linear increase of current observed in the amperogram of Figure 11(B) obtained from the successive additions of 100 µM AA. Anyhow both DA and AA show the lowest detection point was 0.1 µM. Moreover, the anodic current of the sensor reached 95% of the steady-state value within 5 s in case of DA and 4s in case of AA revealed that fast amperometric response behavior.

3.6. Stability and reproducibility.

The stability of the NiO/Graphene modified graphite electrode has been evaluated by measuring its voltammetry response on storage for 1-3 weeks of long term duration. The modified electrode was used for the selective detection of 200 µM DA, in presence of 500 µM Tyr and 5 mM AA in PBS pH 7.0. It is found that the modified electrode could distinguish the **(Fig. not shown)** oxidation peaks of Tyr, DA and AA in their mixture and shows good response to the selective determination of DA retaining 95, 93 and 89% of its initial current response when stored for 1, 2 and 3 weeks respectively.

To ensure the reproducibility of the results, experiments were performed with the same NGMG modified electrode for repeated measurement of 50 µM DA using chronoamperommetry. After each measurement the modified electrode was washed in PBS pH 7.0 and transferred into another standard solution of 50 µM DA to record its oxidation peak current. It is found that the modified electrode lost 9.9 % of initial amperometric response after 15 repeated measurements at a constant Dopamine concentration of 50 µM DA and the step potential applied was 450 mV.

Another experiment was conducted with a single modified electrode and the standard deviation for 10 successive measurements was less than 4% in PBS pH 7.0 solution containing 50 mM DA. This indicates the excellent reproducibility of the modified electrode.

Table 1. Electrochemical parameters on bare graphite and NGMG electrodes during determination of DA in presence of Tyr and AA

Electrode	Parameters	DA in the presence of tyrosine		DA in the presence of AA	
		Dopamine (500 µM)	Tyrosine (500 µM)	Dopamine (200 µm)	AA (5mM)
Bare graphite	E_{pa}/V	0.225	The peaks of DA and Tyr merge to appear as single	Both are oxidized at 0.441V and A single peak for DA and AA was observed	
	I_{pa}/mA	0.015			
NGMG	E_{pa}/V	0.219	0.630	0.285	0.0907
	I_{pa}/mA	0.213	0.129	0.383	0.4337

Table 2. Electrochemical parameters on bare graphite and NGMG electrodes during determination of AA in presence of Tyr

Electrode	Parameters	Tyr in the presence of AA	
		Ascorbic acid (5 mM)	Tyrosine (500 µM)
Bare graphite	E_{pa}/V	0.4236	No specific peak observed
	I_{pa}/mA	0.1247	
NGMG	E_{pa}/V	0.0927	0.6787
	I_{pa}/mA	0.4183	0.3568

4. CONCLUSIONS

The NiO/graphene modified graphite electrode exhibits good electro catalytic activity towards the oxidation of DA, AA and Tyr. Large separations between peak potentials of AA, DA and Tyr allow the detection and determination of Tyr, DA and AA at the modified electrode using cyclic voltammetry and differential pulse voltammetry and chronoamperometry. No electrode fouling was observed upon electro-oxidation of DA in the presence of Tyr or high concentration of AA at the NiO/graphene modified graphite electrode. Simultaneous determination of DA by CV can be well conducted in the presence of high concentration (>100 folds excess) of AA.

5. REFERENCES

1. Kapalka, G. Chapter 4: Substances Involved in Neurotransmission. In: *Nutritional and Herbal Therapies for Children and Adolescents,* 1st Ed., Academic Press is an imprint of Elsevier, London, UK, 2010; pp 74-99, https://doi.org/10.1016/C2009-0-01890-X.

2. Khadjavi, A.; Mannu,F.; Destefanis, P.; Sacerdote, C.; Battaglia, A.; Allasia, M.; Fontana, D.; Frea, B.; Polidoro, S.; Fiorito, G.; Matullo, G.; Pantaleo, A.; Notarpietro, A.;Prato, M.; Castagno, F.; Vineis, P.; Gontero, P.; Giribaldi, G.; Turrini, F. Early diagnosis of bladder cancer through the detection of urinary tyrosine-phosphorylated proteins. *British Journal of Cancer* **2015**, *113*, 469–475, https://doi.org/10.1038/bjc.2015.232.

3. Furukawa, Y.; Kish, S. Tyrosine Hydroxylase Deficiency. In: *GeneReviews® [Internet]*. 1st ed., Adam, M.P.; Ardinger, H.H.; Pagon, R.A.; University of Washington, Seattle, USA, 2008; pp. 1-21.

4. Mohorko, N.; Petelin, A.; Jurdana, M.; Gianni, B.; PraDnikar, Z.J. Elevated Serum Levels of Cysteine and Tyrosine: Early Biomarkers in Asymptomatic Adults at Increased Risk of Developing Metabolic Syndrome. *BioMed Research International* **2015**, 2015, 1-14.

5. Turyan, I.; Frenkel, R.; Sosic, Z. Rapid quantification of tyrosine sulfation in therapeutic proteins. *Anal. Biochem.* **2018,** *549,* 96-98, https://doi.org/10.1016/j.ab.2018.03.001.
6. Ferguson, A.A.; Roy,S.; Kaitlyn, N. K.; Yongsoon, K.; Dumas, K.J.; Ritov, V.B.; Matern, D.; Patrick J. H.; Fisher, A.L.TATN-1 Mutations Reveal a Novel Role for Tyrosine as a Metabolic Signal That Influences Developmental Decisions and Longevity in *caenorhabditis elegans. PLOS Genetics.* **2013**, *9*, 12, 1-22, https://doi.org/10.1371/journal.pgen.1004020.
7. Dalley, J.W.; Roiser, J.P. Dopamine, serotonin and impulsivity. *Neuroscience* **2012**, *215,* 42-58, https://doi.org/10.1016/j.neuroscience.2012.03.065.
8. Kim, D.S.; Kang, E.S.; Baek, S.; Choo, S.S.; Chung, Y.H.; Lee, D.; Min, J.; Kim, T.H. Electrochemical detection of dopamine using periodic cylindrical gold nanoelectrode arrays. *Sci. Rep.* **2018,** *8,* 1-10, https://doi.org/10.1038/s41598-018-32477-0.
9. Devi, N.R.; Kumar, T.V.; Sundramoorthy, A.K. Electrochemically Exfoliated Carbon Quantum Dots Modified Electrodes for Detection of Dopamine Neurotransmitter. *J. Electrochem. Soc.* **2018,** *165,* G3112–G3119, https://doi.org/10.1149/2.0191812jes.
10. Xia, X.; Shen, X.; Du, Y.; Ye, W.; Wang, C. Study on glutathione's inhibition to dopamine polymerization and its application in dopamine determination in alkaline environment based on silver selenide/molybdenum selenide/glassycarbonelectrode. *Sens. Actuators* **2016**, *B237,* 685–692, https://doi.org/10.1016/j.snb.2016.06.154.
11. Üğe, A.; Zeybek, D. K; Zeybek, B. An electrochemical sensor for sensitive detection of dopamine based on MWCNTs/CeO2PEDOT composite. *J. Electroanal. Chem.* **2018**, *813,* 134–142, https://doi.org/10.1016/j.jelechem.2018.02.028.
12. Fazio, E. Molybdenum oxide nanoparticles for the sensitive and selective detection of dopamine. *J. Electroanal. Chem.* **2018,** *814,* 91–96, https://doi.org/10.1016/j.jelechem.2018.02.051.
13. Owesson-White, C.A. Sources contributing to the average extracellular concentration of dopamine in the nucleus accumbens. *J. Neurochem.* **2012**, *121,* 252–262, https://doi.org/10.1111/j.1471-4159.2012.07677.x.
14. How, G.T.S.; Pandikumar, A.; Ming, H.N.; Ngee, L.H. Highly exposed {001} facets of titanium dioxide modified with reduced graphene oxide for dopamine sensing. *Sci. Rep*. **2014**, *4*, 1-8, https://doi.org/10.1038/srep05044.
15. Cheng, M.; Zhang, X.; Wang, M.; Huang, H.; Ma, J. A facile electrochemical sensor based on well-dispersed graphene-molybdenum disulfide modified electrode for highly sensitive detection of dopamine. *J. Electroanal. Chem.* **2017**, *786,* 1–7, https://doi.org/10.1016/j.jelechem.2017.01.012.
16. Massey, L.K.; Liebman, M.; Kynast-Gales, S.A. Ascorbate increases human oxaluria and kidney stone risk. *J. Nutr.* **2005**, *135,* 1673–1677, https://doi.org/10.1093/jn/135.7.1673.
17. Arrigoni, O.; De Tullio, M.C. Ascorbic acid: much more than just an antioxidant. *Biochim. Biophys. Acta.* **2002,** *1569,* 1-9, https://doi.org/10.1016/s0304-4165(01)00235-5.
18. Padayatty, S.J.; Katz, A.; Wang, Y.; Eck, P.; Kwon, O.; Lee, J.H.; Chen, S; Corpe, C.; Dutta. A.; Dutta, S.K.; Levine, M. Vitamin C as an antioxidant: evaluation of its role in disease prevention. *J. Am. Coll. Nutr.* **2003**, *22,* 18-35, https://doi.org/10.1080/07315724.2003.10719272.
19. Alonso,S.; Zamora, L.; Calatayud, M. Determination of tyrosine through a FIA-direct chemiluminescence procedure. *Talanta* **2003,** *60,* 369-376, https://doi.org/10.1016/S0039-9140(03)00099-7.
20. Lee, C.J.; Yang, J. α-Cyclodextrin-modified infrared chemical sensor for selective determination of tyrosine in biological fluids. *Anal. Biochem.* **2006**, *359,* 124-131, https://doi.org/10.1016/j.ab.2006.09.004.
21. Ishii, Y.; Iijima, M.; Umemura,T.; Nishikawa, A.; Iwasaki, Y.; Ito, R.; Saito, K. ;Hirose, M.; Nakazawa, H. Determination of nitrotyrosine and tyrosine by high-performance liquid chromatography with tandem massspectrometry and immunohistochemical analysis in livers of mice administered acetaminophene. *J. Pharm. Biomed. Anal.* **2006**, *41*, 1325-1331, https://doi.org/10.1016/j.jpba.2006.02.045.
22. Huang, Y.; Jiang, X.Y.; Wang, W; Duan, J.P; Chen, G. Separation and determination of L-tyrosine and its metabolites by capillary zone electrophoresis with a wall-jet amperometric detection. *Talanta* **2006,** *70,* 1157-1163, https://doi.org/10.1016/j.talanta.2006.03.009.
23. Ghodsi, J.; Rafati, A. A.; Shoja, Y.; Najafi, M. Determination of dopamine in the presence of uric acid and folic acid by carbon paste electrode modified with CuO nanoparticles/hemoglobin and multi-walled carbon nanotube. *J. Electrochem. Soc.* **2015**, *162*, B69–B74.
24. Schumacher, F. Highly sensitive isotope-dilution liquid-chromatography–electrospray ionization–tandem-mass spectrometry approach to study the drug-mediated modulation of dopamine and serotonin levels in Caenorhabditis elegans. *Talanta* **2015,** *144,* 71–79, https://doi.org/10.1016/j.talanta.2015.05.057.
25. Shen, J.; Sun, C.; Wu, X. Silver nanoprisms-based Tb (III) fluorescence sensor for highly selective detection of dopamine. Talanta. **2017,** *165,* 369–376, https://doi.org/10.1016/j.talanta.2016.12.073.
26. Nurzulaikha, R.; Lim, H.N.; Harrison, I.; Lim, S.S.; Pandikumar, A.; Huang, N.M.; Lim, S.P.; Thien, G.S.H.; Yusoff, N.; Ibrahim, I. Graphene/SnO2 nanocomposite-modified electrode for electrochemical detection of dopamine. *Sens. BioSens. Res.* **2015**, *5,* 42–49, https://doi.org/10.1016/j.sbsr.2015.06.002.
27. Leng, Y.; Xie, K.; Ye, L.; Li, G.; Lu, Z.; He, J. Gold-nanoparticle-based colorimetric array for detection of dopamine in urine and serum. *Talanta* **2015,** *139,* 89–95, https://doi.org/10.1016/j.talanta.2015.02.038.
28. Gao, F.; Liu, L.; Cui,G.; Xu, L.; Wu, X.; Kuang, H.; Xu, C. Regioselective plasmonic nano-assemblies for bimodal sub-femtomolar dopamine detection. *Nanoscale* **2017**, *9*, 223–229, https://doi.org/10.1039/C6NR08264E.
29. Carrera, V.; Sabater, E.; Vilanova, E.; Sogorb, M.A. A simple and rapid HPLC–MS method for the simultaneous determination of epinephrine, norepinephrine, dopamine and 5-hydroxytryptamine: Application to the secretion of bovine chromaffin cell cultures. *J. Chromatogr. B*. **2007**, *847,* 88–94, https://doi.org/10.1016/j.jchromb.2006.09.032.
30. Chen, J.L.; Yan, X.P; Meng, K.; Wang, S.F. Graphene Oxide Based Photoinduced Charge Transfer Label-Free Near-Infrared Fluorescent Biosensor for Dopamine. *Anal. Chem.* **2011**, *83,* 8787–8793, https://doi.org/10.1021/ac2023537.
31. Khattar, R.; Mathur, P. 1-(Pyridin-2-ylmethyl)-2-(3-(1-(pyridin-2-ylmethyl)benzimidazol-2-yl) propyl) benzimidazole and its copper(II) complex as a new fluorescent sensor for dopamine (4-(2-aminoethyl)benzene-1,2-diol). *Inorg. Chem. Commun.* **2013**, *31,* 37–43, https://doi.org/10.1016/j.inoche.2013.02.015.
32. Suntornsuk, L.; Gritsanapun, W.; Nilkamhank, S.; Paochom, A. Quantitation of vitamin C content in herbal juice using direct titration. *J Pharm Biomed Anal.* **2002,** *28*, 849–855, https://doi.org/10.1016/S0731-7085(01)00661-6.

33. Dai, H.; Wu, X.P.; Wang, Y.M.; Zhou, W.C.; Chen, G.N. An electrochemiluminescent biosensor for vitamin C based on inhibition of luminal electro-chemiluminescence on graphite/poly(methyl metha crylate) composite electrode. *Electro chim Acta.* **2008**, *53,* 5113–5117. https://doi.org/10.1016/j.electacta.2008.02.044.
34. Tai, A.; Gohda, E. Determination of ascorbic acid and its related compounds in foods and beverages by hydrophilic interaction liquid chromatography. *J Chromatogr B.* **2007**, *853,* 214–220, https://doi.org/10.1016/j.jchromb.2007.03.024.
35. Wu, X.; Diao, Y.X.; Sun, C.X.; Yang, J.H.; Wang, Y.B.; Sun, S.N. Fluorimetric determination of ascorbic acid with ophenylenediamine. *Talanta* **2003**, *59*, 95–99, https://doi.org/10.1016/S0039-9140(02)00475-7.
36. Kumar, S.A.; Lo, P.H.; Chen, S.M. Electrochemical selective determination of ascorbic acid at redox active polymer modified electrode derived from direct blue 71. *Biosens Bioelectron*. **2008**, *24*, 518–523, https://doi.org/10.1016/j.bios.2008.05.007.
37. Wen, D.; Guo, S.J.; Dong, S.J.; Wang, E.K. Ultrathin Pd nanowire as a highly active electrode material for sensitive and selective detection of ascorbic acid. *Biosens Bioelectron.* **2010**, *26*, 1056–1061, https://doi.org/10.1016/j.bios.2010.08.054.
38. Khan, A.; Khan, M.I.; Iqbal, Z.; Shah,Y.; Ahmad, L.; Nazir, S.; Watson, D.G.; Khan, J.A.; Nasir, F.; Khan, A.; Ismail. A new HPLC method for the simultaneous determination of ascorbic acid and aminothiols in human plasma and erythrocytes using electrochemical detection. *Talanta* **2011**, *84,* 789–801, https://doi.org/10.1016/j.talanta.2011.02.019.
39. Danielle, W.K.; Gabriel, L.B.; Mika, E.M.; David, E.C. Electrochemical Sensors and Biosensors. *Anal. Chem.* **2012**, *84,* 685–707, https://doi.org/10.1021/ac202878q.
40. Mahmoud, L.; Edward, H.S.; Shana, O.K. Electrochemical Methods for the Analysis of Clinically Relevant Biomolecules. *Chem. Rev.* **2016**, *116,* 9001-9090, https://doi.org/10.1021/acs.chemrev.6b00220.
41. Zahra, T.A.; Oana, H.; Cecilia, C.; Mohammad, M.A.; Giovanna, M. Latest Trends in Electrochemical Sensors for Neurotransmitters: A Review. *Sensors* **2019**, *19*, 1-30, https://doi.org/10.3390/s19092037.
42. Bhakta, A.K.; Mascarenhas, R.J.; D'Souza, O.J ; Satpati, A.K.; Detriche, S.; Mekhalif, Z.; Dalhalle, J. Iron nanoparticles decorated multi-wall carbon nanotubes modified carbon paste electrode as an electrochemicalsensor for the simultaneous determination of uric acid in the presence of ascorbic acid, dopamine and L-tyrosine. *Materials Science and Engineering C* **2015**, *57,* 328–337, http://dx.doi.org/10.1016/j.msec.2015.08.003.
43. Manjunatha, H.; Nagaraju, D.H.; Suresh, G.S.; Venkatesha, T.V. Detection of Uric Acid in the Presence of Dopamine and High Concentration of Ascorbic Acid Using PDDA Modified Graphite Electrode. *Electroanalysis* **2009**, *21,* 2198–2206, https://doi.org/10.1002/elan.200904662.
44. Wan, Q.L.; Zhiqiang, G. Metal Oxide Nanoparticles in Electroanalysis. Electroanalysis **2015**, *27,* 1–18, https://doi.org/10.1002/elan.201500024.
45. Tooley, C.A.; Gasperoni,C.H.; Marnoto. S.; Halpern, J.M. Evaluation of Metal Oxide Surface Catalysts for the Electrochemical Activation of Amino Acids. *Sensors.* **2018**, *18,* 1-10, https://doi.org/10.3390/s18093144.
46. Yang, J.; Yu, J.H.; Strickler, J.R.; Chang, W.J.; Gunasekaran, S. Nickel nanoparticle-chitosan-reduced graphene oxide-modified screen-printed electrodes for enzyme-free glucose sensing in portable microfluidic devices. *Biosens. Bioelectron*. **2013**, *47,* 530-538, https://doi.org/10.1016/j.bios.2013.03.051.
47. Liu, B.; Luo, L.; Ding, Y.; Si, X.; Wei, Y.; Ouyang, X.; Xu, D. Differential pulse voltammetric determination of ascorbic acid in the presence of folic acid at electro-deposited NiO/graphene composite film modified electrode. *Electrochim. Acta* **2014**, *142,* 336–342, https://doi.org/10.1016/j.electacta.2014.07.126.
48. Yang, L.; Wangn, G.; Liu,Y.; Wang, M. Development of a biosensor based on immobilization of acetylcholinesterase on NiO nanoparticles–carboxylic graphene–nafion modified electrode for detection of pesticides. *Talanta* **2013**, *113*, 135-141, https://doi.org/10.1016/j.talanta.2013.03.025.
49. Dong, S.; Zhang, P.; Liu, H.; Li, N.; Huang, T. Direct electrochemistry and electrocatalysis of hemoglobin in composite film based on ionic liquid and NiO microspheres with different morphologies. *Biosens. Bioelectron.* **2011**, *26,* 4082-4087, https://doi.org/10.1016/j.bios.2011.03.039.
50. Hong, Y.Y.; Zhang, H.J.; Huang, S.; Gao, X.; Shan, S.S.; Wang, Z.; Wang, W.Q.; Gua, N.E.H. A novel non-enzymatic dopamine sensors based on NiO-reduced graphene oxide hybrid nanosheets. *Journal of Materials Science: Materials in Electronics* **2019**, *30,* 5000–5007, https://doi.org/10.1007/s10854-019-00796-1.
51. Asghar, P.; Akbarzadeh-Torbati, N.; Beitollahi, H. Rapid and Sensitive Electrochemical Monitoring of Tyrosine Using NiO Nanoparticles Modified Graphite Screen Printed Electrode. Int. *J. Electrochem. Sci.* **2019**, *14,* 1556–1565, https://doi.org/10.20964/2019.02.42.
52. Wang, C.; Xu, J.; Yuen, M.F.; Zhang, J.; Li, Y.; Chen, X.; Zhang, W. Hierarchical composite electrodes of nickel oxide nanoflake 3D graphene for high-performance pseudocapacitors. *Adv. Func. Mater.* **2014,** *24,* 6372–6380, https://doi.org/10.1002/adfm.201401216.
53. Pumera, M. Graphene-based nanomaterials and their electrochemistry. *Chem. Soc. Rev.* **2010**, *39,* 4146–4157, https://doi.org/10.1039/C002690P.
54. Tang, L.; Wang, J.; Loh. K.P. Graphene-Based SELDI Probe with Ultrahigh Extraction and Sensitivity for DNA Oligomer. *J. Am. Chem. Soc.* **2010**, *132,* 10976-10977, https://doi.org/10.1021/ja104017y.
55. Li, D.; Müller, M.B; Gilje, S.; Kaner, R.B.; Wallace, G.G. Processable aqueous dispersions of graphene nanosheets. *J. Nat. Nanotechnol.* **2008**, *3,* 101-105, https://doi.org/10.1038/nnano.2007.451.
56. Ohno, Y.; Maehashi, K.; Yamashiro, Y.; Matsumoto, K. Electrolyte-Gated Graphene Field-Effect Transistors for Detecting pH and Protein Adsorption. *J. Nano Letters* **2009,** *9*, 3318-3322, https://doi.org/10.1021/nl901596m.
57. Schedin, F.; Geim, A.K.; Morozov, S.V.; Hill, E.W.; Blake, P.; Katsnelson, M.I.; Novoselov, K.S. Detection of individual gas molecules adsorbed on graphene. *J. Nature Materials* **2007**, *6,* 652-655, https://doi.org/10.1038/nmat1967.
58. Mohanty, N.; Berry, V. Graphene-Based Single-Bacterium Resolution Biodevice and DNA Transistor: Interfacing Graphene Derivatives with Nanoscale and Microscale Biocomponents. *J. Nano Letters* **2008**, *8,* 4469-4476, https://doi.org/10.1021/nl802412n.
59. Bagheri, H.; Arab, S.M.; Khoshsafar, H.; Afkhami, A. A novel sensor for sensitive determination of atropine based on a Co_3O_4-reduced graphene oxide modified carbon paste electrode. *New J. Chem.* **2015**, *39,* 3875-388, https://doi.org/10.1039/C5NJ00133A.
60. Tajik, S.; Taher, M.A.; Beitollahi, H. Application of a new ferrocene-derivative modified-graphene paste electrode for simultaneous determination of isoproterenol, acetaminophen and theophylline. *Sens. Actuators B.* **2014**, *197,* 228-236, https://doi.org/10.1016/j.snb.2014.02.096.
61. Afkhami, A.; Khoshsafar, H.; Bagheri, H.; Madrakian, T. Facile simultaneous electrochemical determination of codeine

and acetaminophen in pharmaceutical samples and biological fluids by graphene–$CoFe_2O_4$ nancomposite modified carbon paste electrode. *Sens. Actuators B.* **2014**, *203,* 909-918, https://doi.org/10.1016/j.snb.2014.07.031.
62. Beitollahi, H.; Hamzavi, M.; Torkzadeh-Mahani, M. Electrochemical determination of hydrochlorothiazide and folic acid in real samples using a modified graphene oxide sheet paste electrode. *Mater. Sci. Engin. C* **2015**, *52,* 297-305, https://doi.org/10.1016/j.msec.2015.03.031.
63. Anuprathap, M.U.; Srivastava, R. Synthesis of $NiCo_2O_4$ and its application in the electrocatalytic oxidation of methanol. *NanoEnergy* **2013**, *2,* 1046-1053, https://doi.org/10.1016/j.nanoen.2013.04.003.
64. Shanaj, B.R.; John, X.R. Effect of Calcination Time on Structural, Optical and Antimicrobial Properties of Nickel Oxide Nanoparticles. *J Theor Comput Sci.* **2016**, *3,* 1-10, https://doi.org/10.4172/2376-130X.1000149.
65. Alagiri, M; Ponnusamy, S; Muthamizhchelvan, C. Synthesis and characterization of NiO nanoparticles by sol–gel method. *J Mater Sci: Mater Electron.* **2012**, *23,* 728–732, https://doi.org/10.1007/s10854-011-0479-6.
66. Fayemi, O.E.; Adekunle, A.S.; Kumara Swamy, B.E.; Ebenso, E.E. Electrochemical sensor for the detection of dopamine in real samples using polyaniline/NiO, ZnO, and Fe3O4 nanocompositeson glassy carbon electrode. *Journal of Electroanalytical Chemistry* **2018,** *818,* 236-249, https://doi.org/10.1016/j.jelechem.2018.02.027.
67. Valenzuela, M.V.; Huerta, F.; Morallón, E.; Montilla, F. Affinity of Electrochemically Deposited Sol–Gel Silica Films towards Catecholamine Neurotransmitters. *Sensors* **2019**, *19,* 1-15., https://doi.org/10.3390/s19040868.
68. Xu, Z.; Gao, N.; Chen.H.; Dong, S. Biopolymer and carbon nanotubes interfacprepared by self-assembly for studying the electrochemistry of microperoxidase-11. *Langmuir* **2015**, *2,* 10808-10813, https://doi.org/10.1021/la051445.
69. Bard, A.J.; Faulkner, L.R. Electrochemical Methods, Fundamentals and Applications. 2nd Ed. Wiley, New York.2006
70. Laviron, E. General expression of the linear potential sweep voltammogram in the case of diffusionless electrochemical systems. *J. Electroanal. Chem. Interfacia Electrochem.* **1979,** *101*, 19–28, https://doi.org/10.1016/S0022-0728(79)80075-3.
71. Yang, S.; Li, G.; Yin, Y.; Yang, Y.; Li, J.; Qu, L. Nano-sized copper oxide/multi-wall carbon nanotube/Nafion modified electrode for sensitive detection of dopamine. *Journal of Electroanalytical Chemistry* **2013**, *703,* 45–51, http://dx.doi.org/10.1016/j.jelechem.2013.04.020.
72. Hao, C.; Changdong, C.; Shuai, Z. Electrochemical Behavior and Sensitive Determination of L-Tyrosine with a Gold Nanoparticles Modified Glassy Carbon Electrode. *Analytical sciences* **2009,** *25,* 1221-1225, https://doi.org/10.2116/analsci.25.1221.
73. Jamal, M.; Chakrabarty, S.; Han, S.; David, M.; Yousuf, M.A.; Furukawa, H.; Ajit, K.; Kafil, M.R. A non enzymatic glutamate sensor based on nickel oxide nanoparticle. *Microsystem Technologies* **2018,** *24,* 4217–4223. https://doi.org/10.1007/s00542-018-3724-6.
74. Ghoreishi, S.M.; Behpour, M.; Delshad, M.; Khoobi,A. Electrochemical determination of tyreosine in the presence of uric acid at a carbon paste electrode modified with multi-walled carbon nanotubes enhanced by sodium dodecyl sulfate. *Cent. Eur. J. chem.* **2012,** *10,* 1824-1829, https://doi.org/10.2478/s11532-012-0119-x.
75. Majid, S.; Rhazi, M.E.; Amine, A.; Brett, C.M.A. An amperometric method for the determination of trace mercury (II) by formation of complexes with L-tyrosine. *Analytica Chimica Acta* **2002**, *464,* 123-133, https://doi.org/10.1016/S0003-2670(02)00422-1.

6. ACKNOWLEDGEMENTS

Authors gratefully acknowledge the financial support for this work by Department of Science and Technology (DST-SERB)-Project No., ECR/2016/000644, Govt. of India. Authors are also grateful to the Management of GITAM (Deemed to be University), Bangaluru Campus for the support and encouragement.

© 2020 by the authors. This article is an open access article distributed under the terms and conditions of the Creative Commons Attribution (CC BY) license (http://creativecommons.org/licenses/by/4.0/).